Electronic properties for icosahedral and amorphous phases in the Mg-Zn-Al alloy system

1989 J. Phys.: Condens. Matter 1 4087

(http://iopscience.iop.org/0953-8984/1/26/005)

J. Phys.: Condens. Matter 1 (1989) 4087–4098. Printed in the UK

Electronic properties for icosahedral and amorphous phases in the Mg–Zn–Al alloy system

T Matsuda†, I Ohara†, H Sato†, S Ohashi‡ and U Mizutani‡

† Department of Physics, Aichi University of Education, Kariya, Aichi 448, Japan

‡ Department of Crystalline Materials Science, Nagoya University, Furo-cho, Chikusa-ku, Nagoya 464-01, Japan

Received 30 November 1988

Abstract. Low-temperature specific heat and various electron transport properties have been measured for the icosahedral $Mg_{32}Al_{17}Zn_{32}$ and six alloys with the formula $(Mg_{1-x}Al_x)_{65}Zn_{35}$ ($x = 0$, 0.05, 0.1, 0.15, 0.2 and 0.3), all of which were fabricated in the ribbon form by the melt-spinning technique. This series of Mg–Al–Zn alloys covers the composition range over which the amorphous single phase is gradually taken over by the icosahedral quasicrystalline phase with increasing Al content. The density of states at the Fermi level turns out to be close to the free-electron value for both amorphous and icosahedral phases. As far as the resistivity is concerned, no significant difference is observed between these two phases. However, the Hall coefficient and the thermo-electric power for the icosahedral phase exhibit unique temperature dependences apparently inherent to the quasicrystalline structure and, hence, their behaviour is sharply distinguished from that in the amorphous phase.

1. Introduction

Quasicrystals diffract electrons or x-rays to yield Bragg spots like a single crystal but with a symmetry incompatible with the ordinary crystal translational order. This unique feature is of particular interest not only from the viewpoint of structural analysis but also because of its effect on the electron transport properties. We naturally address ourselves to the question as to whether the electron transport mechanism resembles that in amorphous alloys or in crystals. As far as non-magnetic amorphous alloys are concerned, we have reached such a stage that the electron transport mechanism can be described in a unified manner, by using the value of resistivity as a key parameter (Mizutani 1988a, b). Therefore, it is now timely to extend the study of the electron transport properties to quasicrystals and to discuss the scattering mechanism by making a direct comparison with the results for similar amorphous alloys.

After the discovery of Al–Mn quasicrystals by Shechtman *et al* (1984), a large number of alloys have been identified as forming the icosahedral quasicrystal structure. Apart from the Al–Mn-type quasicrystals, another family of icosahedral alloys exists consisting only of simple elements, which includes Mg–Al–Zn (Ramachandrarao and Sastry 1985, Baxter *et al* 1987), Mg–Al–Cu (Sastry *et al* 1986), Mg–Ga–Zn (Chen and Inoue 1987), Mg–Al–Ag (Chen *et al* 1987, Inoue *et al* 1988) and Al–Li–Cu (Ball and Lloyd 1985). The electron conduction in these alloys is exclusively dominated by s or p electrons at the Fermi level and is entirely free from the magnetic effect as well as from the d-electron

0953-8984/89/264087 + 12 $02.50

Table 1. Low-temperature specific heat data for melt-spun $(Mg_{1-x}Al_x)_{65}Zn_{35}$ and $Mg_{32}Al_{17}Zn_{32}$. γ_{exp}, α and δ are the coefficients for the equation $C = \gamma T + \alpha T^3 + \delta T^5$ (see § 3.2). Θ_D is the Debye temperature. (I) and (C) refer to the icosahedral and the Frank–Kasper phases respectively.

Al composition x	γ_{exp} (mJ mol^{-1} K^{-2})	α (10^{-2} mJ mol^{-1} K^{-4})	Θ_D (K)	δ (10^{-4} mJ mol^{-1} K^{-6})
0	1.03 ± 0.01	7.95 ± 0.15	290 ± 2	2.1 ± 0.3
0.05	0.99 ± 0.01	7.08 ± 0.12	302 ± 2	1.3 ± 0.3
0.10	0.97 ± 0.01	6.31 ± 0.08	313 ± 1	1.5 ± 0.2
0.15	0.93 ± 0.01	6.08 ± 0.01	317 ± 1	0.4 ± 0.2
0.20	0.93 ± 0.01	5.97 ± 0.01	319 ± 1	0.4 ± 0.2
0.30	0.99 ± 0.01	3.7 ± 0.1	373 ± 4	4.2 ± 0.4
$Mg_{32}Al_{17}Zn_{32}$ (I)	0.93 ± 0.01	3.6 ± 0.1	378 ± 4	3.4 ± 0.4
$Mg_{32}Al_{17}Zn_{32}$ (C)	1.04 ± 0.01	6.3 ± 0.1	356 ± 2	1.9 ± 0.2

contribution. Baxter *et al* (1987) studied the temperature and magnetic field dependence of the electrical resistivity on single-phase icosahedral $Mg_{32}(Al_{1-x}Zn_x)_{49}$ at $x = 0.5$ and $x = 0.69$ and discussed the data obtained below 20 K on the basis of the theory of quantum corrections to electron transport in disordered systems. Graebner and Chen (1987) reported the specific heat data for the Frank–Kasper cubic, icosahedral and amorphous phases of $Mg_3Zn_3Al_2$ in the temperature range 0.04–5 K and revealed that the density of states (DOS) at the Fermi level is close to the free-electron value for all three phases. A choice of such electronically simple alloys is critically important for extracting information about the interaction of conduction electrons with quasi-periodic arrays of ions and to make a direct comparison with the corresponding amorphous structure. In the present study, we selected the Mg–Zn–Al alloy system, where both amorphous and icosahedral single phases can be produced by changing the Al concentration. We studied a change in the electron transport properties accompanied with the structural change from a glass to quasicrystal.

2. Experimental procedure and results

All alloy ingots $Mg_{32}Al_{17}Zn_{32}$ and $(Mg_{1-x}Al_x)_{65}Zn_{35}$ ($x = 0$, 0.05, 0.10, 0.15, 0.20 and 0.30) were prepared by repeated induction melting of constituent elements 99.999% Al, 99.999% Zn and 99.95% Mg in a high-purity graphite crucible under a pressurised helium atmosphere. Small pieces of the alloy ingot were rapidly solidified by melt spinning onto a copper wheel at a tangential velocity of 62 m s^{-1}. The resulting ribbons were typically 2 mm wide and about 10 μm thick. With increasing Al content, the melt-spun ribbon becomes very brittle and its length is limited to only 10–50 mm.

Both amorphous and quasicrystal structures were identified by using an ordinary x-ray diffractometer with Cu Kα radiation and a transmission electron microscope (TEM). The low-temperature specific heats were measured in the temperature range 1.5–6 K. The sample, its weight being about 2 g, was compacted in a gold-plated copper container, the contribution of which to the heat capacity was subtracted from the total. The numerical data are summarised in table 1.

The mass density was measured by Archimedes' method. The determination of the density for alloys containing the quasicrystal phase was extremely difficult, because small

pieces of flakes escaped from tiny holes in a platinum basket when immersed into a xylene bath. Hence, the density was measured using as-prepared ingots except for the ductile amorphous ribbon sample $Mg_{65}Zn_{35}$. We consider the error caused by this substitution to be of minor importance. The electrical resistivity ρ was measured in the temperature range 1.5–300 K, using a standard DC method. The Hall coefficient R_H was also measured in the range 77–300 K. A major error in determining the value of ρ and R_H at room temperature originated from the lack of uniformity in ribbon thickness, the average value of which was determined by measuring the value for more than five identical specimens. The thermo-electric power measurements were performed using the integral method in the temperature range 78–570 K. The details are described elsewhere (Matsuda *et al* 1986).

The crystallisation behaviour was monitored by measuring the resistivity and the differential thermal analysis (DTA) curve in the range 300–700 K at a heating rate of 10 K min^{-1}. The structural change associated with the transformation was studied at room temperature by x-ray diffraction on a specimen heated up at the same rate just above the critical temperature at which the DTA curve exhibits an exothermic peak.

Numerical data including electron transport properties, the average atomic weight A, the mass density d and the crystallisation temperature T_x are listed in table 2.

3. Discussion

3.1. Structure and crystallisation behaviour

Figure 1 shows the x-ray diffraction patterns for $Mg_{32}Al_{17}Zn_{32}$ and a series of $(Mg_{1-x}Al_x)_{65}Zn_{35}$ alloys. It has been reported that the icosahedral single phase of the best quality is obtained at the alloy composition $Mg_{32}Al_{17}Zn_{32}$ (Yamane *et al* 1987, Shibuya *et al* 1988). The x-ray diffraction lines for all samples except $x = 0$ can be indexed in terms of the icosahedral structure. It can be seen, however, that the Bragg peaks become progressively reduced in intensity and broadened with decreasing Al content and that a halo centred at about $2\theta = 37°$ superimposes. This indicates that not only does the amount of the icosahedral phase increase with increasing Al content, but also its quasi-crystallinity improves and that the alloys with Al composition $0.05 \leq x \leq 0.2$ are essentially a mixture of amorphous and icosahedral phases.

The TEM observations were performed on most of the present samples studied. It turned out that the $Mg_{32}Al_{17}Zn_{32}$ alloy consists of an icosahedral single phase characterised by the same features as observed by Ramachandrarao and Sastry (1985). The average grain size was about 2 μm, no trace of amorphous or other crystalline phases being detected. The sample with $x = 0.3$ was found to be essentially an icosahedral single phase, although the grain size was less than 0.5 μm and the grain boundary was less clear. The grain size for alloys with $x = 0.2$ and 0.1 was further reduced and this made it difficult to take a diffraction pattern within a single grain. Instead, halo rings appeared in the electron diffraction pattern.

The DTA data are shown in figure 2 for three representative alloys with $x = 0$ and 0.3 and $Mg_{32}Al_{17}Zn_{32}$. The crystallisation temperature T_x was determined as the onset of the first exothermic peak and is marked by a triangle in figure 2. The heat evolved upon crystallisation is found to decrease with increasing Al content. This suggests that the local atomic structure for the icosahedral phase more closely resembles that for the crystallised phase than that for the amorphous phase. Indeed, the x-ray diffraction

Table 2. Electronic properties of melt-spun $(Mg_{1-x}Al_x)_{65}Zn_{35}$ and $Mg_{32}Al_{17}Zn_{32}$ alloys. TCR and TCH are defined as $[|1/R_H|(dR_H/dT)]_{300K}$, respectively. Other variables are defined in the text.

x	e/a	A g mol^{-1}	d g/cm^{-3}	T_x (K)	ρ_{300K} $\mu\Omega$ cm	TCR (10^{-4} K^{-1})	R_H (10^{-11} m^3 A^{-1} s^{-1})	R_H^{fc} (10^{-11} m^3 A^{-1} s^{-1})	TCH (10^{-4} K^{-1})	$\lvert\Delta R_H/R_H^{fc}\rvert$ (%)	S_{300K} (μV K^{-1})
0	2.0	38.6778	3.154	390	56 ± 2	−3.77	−5.6 ± 0.3	−6.35	−1.07	12	0.16
0.05	2.035	38.7647	(3.20)	395	60 ± 2	−4.53	−5.4 ± 0.3	−6.17		12	−0.37
0.10	2.065	38.8517	3.255	404	69 ± 2	−5.08	−4.8 ± 0.4	−5.99	−1.04	20	−1.17
0.15	2.0975	38.9387	(3.305)	406	72 ± 2		−5.7 ± 0.5	−5.82		2	−2.40
0.20	2.13	39.0257	3.339	418	79 ± 3	−6.07	−6.6 ± 0.7	−5.68	−1.14	16	−4.05
0.30	2.195	39.1997	3.452	455	96 ± 3	−3.99	−11.6 ± 0.5	−5.36	10.3	116	−6.47
$Mg_{32}Al_{17}Zn_{32}$	2.17	41.0899	3.705	520	103 ± 3	−3.62	−12.2 ± 1.5	−5.29	7.0	131	−7.27

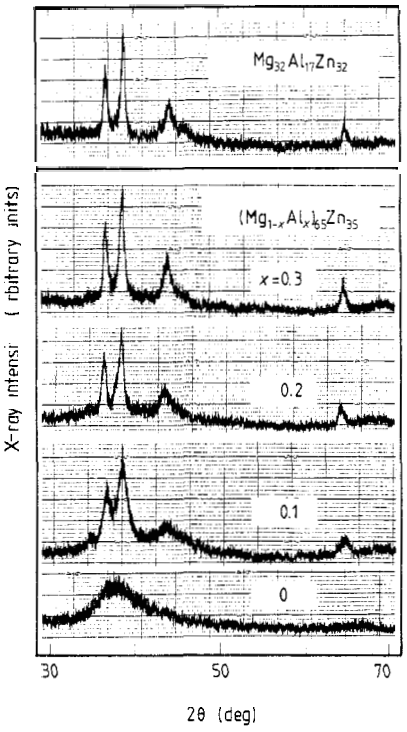

Figure 1. X-ray diffraction patterns for melt-spun $Mg_{32}Al_{17}Zn_{32}$ and $(Mg_{1-x}Al_x)_{65}Zn_{35}$ alloys.

analysis revealed that both $Mg_{32}Al_{17}Zn_{32}$ and the alloy with $x = 0.3$ after crystallisation consist of the Frank–Kasper cubic single phase, the local structure of which is similar to the icosahedral quasicrystal structure. On the other hand, the amorphous alloy $Mg_{65}Zn_{35}$ exhibits two distinctive exothermic peaks. The first one corresponds to the formation of the metastable orthorhombic phase $\mathbf{Mg_{51}Zn_{20}}$ and the second to its decomposition into α-Mg and **Mg**Zn compound (Matsuda and Mizutani 1981).

The transformation behaviour was also monitored by the resistivity measurements. The results are shown in figure 3. The value of T_x deduced from the DTA data is marked as a triangle in figure 3. It can be seen that the crystallisation of the amorphous alloy $Mg_{65}Zn_{35}$ into $Mg_{51}Zn_{20}$ accompanies a small drop in resistivity and that its further decomposition into α-Mg and **Mg**Zn brings about a much larger drop in resistivity at about 520 K. With increasing Al content, a change in resistivity at T_x becomes less clear. As mentioned above, the crystallisation of the icosahedral phase results in the formation of the Frank–Kasper phase. The resistivity of the icosahedral alloys does not show any noticeable change at T_x but it gradually decreases with further increase in temperature. The x-ray diffraction measurements revealed that no new crystalline phases appear above T_x and the crystallinity of the Frank–Kasper phase is simply improved with increasing temperature.

3.2. Electronic structure

Information about the electronic structure of the icosahedral quasicrystals is derived from the low-temperature specific heat data. All the data are found to fall almost on a

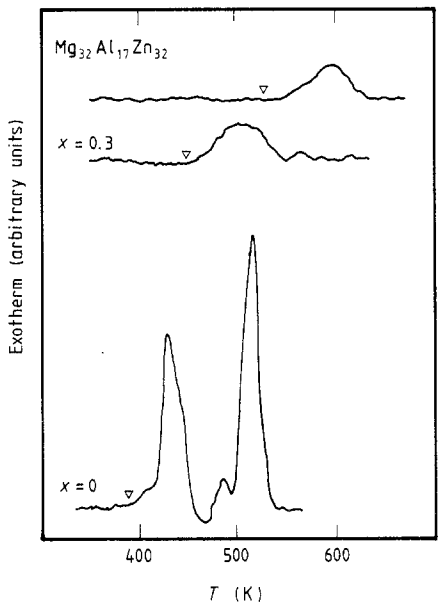

Figure 2. DTA curves for melt-spun $Mg_{32}Al_{17}Zn_{32}$ and $(Mg_{1-x}Al_x)_{65}Zn_{35}$ alloys. Inverted triangles refer to the crystallisation temperature T_x.

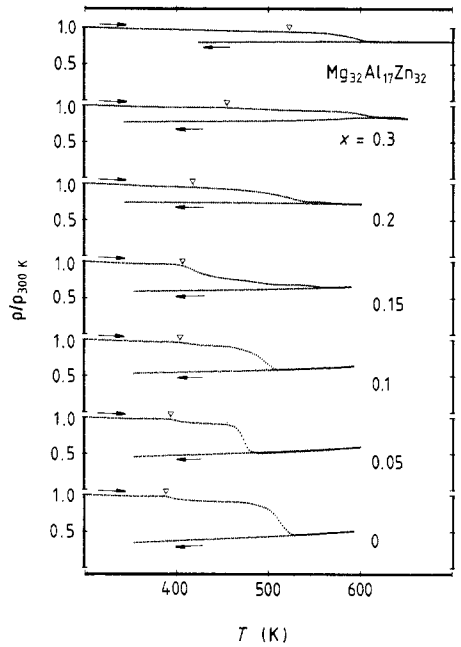

Figure 3. Temperature dependence of the electrical resistivity normalised with respect to that at 300 K for melt-spun $Mg_{32}Al_{17}Zn_{32}$ and $(Mg_{1-x}Al_x)_{65}Zn_{35}$ alloys. Inverted triangles refer to the crystallisation temperature T_x.

straight line in the C/T versus T^2 plot, regardless of whether they refer to the glassy state or the quasicrystalline one. The data are fitted to an ordinary equation

$$C = \gamma T + \alpha T^3 + \delta T^5 \tag{1}$$

where γ is the electronic specific heat coefficient and α and δ are the lattice specific heat coefficients. The Debye temperature Θ_D is calculated from α.

The experimentally derived γ_{exp}, together with the Debye temperature, are plotted in figure 4 as a function of Al concentration. The free-electron value γ_f is calculated by using the measured mass density and the average electron concentration, the latter being derived under the assumption that Mg, Zn and Al donate 2, 2 and 3 valence electrons per atom, respectively. As is seen in figure 4, the value of γ_{exp} is essentially independent of the Al concentration and is very close to the free-electron value. The validity of the free-electron model for the amorphous Mg–Zn alloys has been discussed in the literature (Mizutani and Mizoguchi 1981, Matsuda *et al* 1984, Hafner *et al* 1988). We confirmed that the free-electron model is also valid for the icosahedral quasicrystals with $x = 0.3$ and for $Mg_{32}Al_{17}Zn_{32}$. A similar conclusion was drawn by Graebner and Chen (1987), who measured the electronic specific heats for both crystalline and icosahedral phases of $Mg_{37.5}Al_{25}Zn_{37.5}$. It may be of interest to mention that Marcus (1986) calculated the density of states for the three-dimensional quasi-periodic lattice and found the results to be similar to those for an ordered lattice.

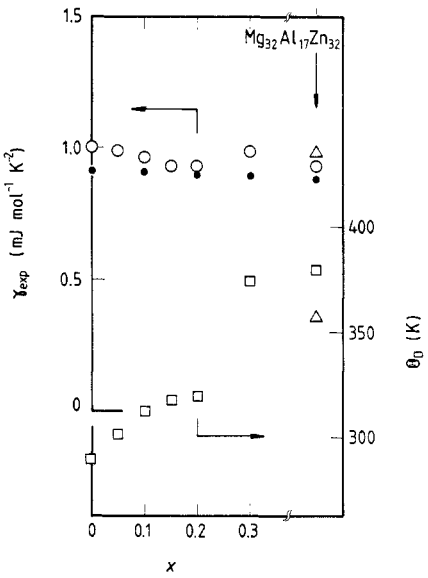

Figure 4. ○, experimentally derived electronic specific heat coefficient γ_{exp}; □, Debye temperature Θ_D, for melt-spun $Mg_{32}Al_{17}Zn_{32}$ and $(Mg_{1-x}Al_x)_{65}Zn_{35}$ alloys. △, data for the Frank–Kasper phase. ●, free-electron values of γ.

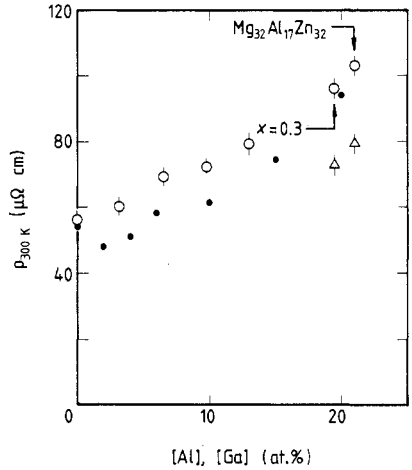

Figure 5. Resistivity at 300 K as a function of Al or Ga content for: ○, melt-spun $Mg_{32}Al_{17}Zn_{32}$ and $(Mg_{1-x}Al_x)_{65}Zn_{35}$ alloys; ●, amorphous $Mg_{70}Zn_{30-x}Ga_x$ alloys (after Matsuda *et al* 1984). △, data for the Frank-Kasper phase.

3.3. Electron transport properties

The resistivities at 300 K as functions of Al content are plotted in figure 5 for the alloys studied. For comparison, the data for amorphous alloys $Mg_{70}Zn_{30-x}Ga_x$ (Matsuda *et al* 1984) are incorporated, although the alloy formula is slightly different. The values of ρ increase with increasing Al (or Ga) content in both alloy systems and fall on similar curves. In particular, the values of ρ for the alloys containing 20 at.% trivalent atoms Al and Ga are quite similar to each other, irrespective of the icosahedral quasicrystal or the amorphous phase. This means that the scattering cross section for divalent Mg and Zn is more or less the same and that the addition of trivalent Al or Ga to the isodivalent Mg–Zn matrix is essential in raising the resistivity. In other words, whether the alloy is in the glassy state or in the quasicrystalline one is less important.

Included in figure 5 are the resistivities for the well crystallised Frank–Kasper phase. The value of ρ is reduced to about 70% of that of the corresponding icosahedral phase. We also stressed above that there is no essential difference in the magnitude of ρ between the icosahedral and amorphous phases. Our observations are in serious disagreement with the data reported by Graebner and Chen (1987), who reported not only an unusually large ρ of 380 $\mu\Omega$ cm for an amorphous phase but also a higher value (90 $\mu\Omega$ cm) for the Frank–Kasper phase than for the icosahedral phase (79 $\mu\Omega$ cm). It may be noted here that they prepared the amorphous sample by the sputtering technique. This might be responsible for the extremely large resistivity they observed.

We now direct our attention to the temperature dependence of the electrical resistivity over the range 1.5–300 K. The data are shown in figure 6 for a series of alloys $(Mg_{1-x}Al_x)_{65}Zn_{35}$. The amorphous alloy $Mg_{65}Zn_{35}$ exhibits a small and broad maximum at about 30 K with a subsequent decrease in resistivity with increasing temperature. This

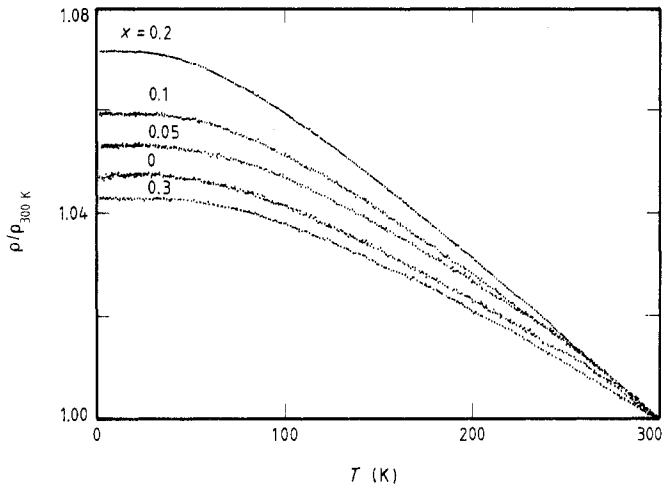

Figure 6. Temperature dependence of the electrical resistivity normalised with respect to that at 300 K for melt-spun $(Mg_{1-x}Al_x)_{65}Zn_{35}$ alloys.

is consistent with the earlier data reported by Matsuda and Mizutani (1982). The icosahedral quasicrystal with $x = 0.3$ also possesses an overall temperature dependence similar to that for the amorphous alloy with $x = 0$, except that the resistivity maximum has disappeared. Note that the resistivity in the quasicrystal with $x = 0.3$ is almost twice that in the amorphous alloy $Mg_{65}Zn_{35}$. As mentioned above, the amorphous alloy $Mg_{70}Zn_{10}Ga_{20}$ also possesses a resistivity comparable to that in the present icosahedral alloy with the absence of the resistivity maximum (Matsuda *et al* 1984). Hence, it is confirmed that no striking features characteristic of the quasicrystal have been observed, as far as the resistivity behaviour is concerned, and that the overall behaviour is quite similar to that found in the amorphous alloys.

According to the analysis by Mizutani (1988a, b), the presence of the resistivity maximum and its shift to absolute zero with increasing resistivity can be understood within the framework of the generalised Faber–Ziman theory based on the Boltzmann transport equation. We therefore believe that the electron transport properties in the relatively low-resistivity ($\rho < 100\ \mu\Omega$ cm) quasicrystals can also be described within the framework of the generalised Faber–Ziman theory without invoking sizeable quantum corrections.

3.4. Hall coefficient

Figure 7 shows the temperature dependences of the Hall coefficient R_H for the alloys studied. In contrast to the resistivity behaviour described in § 3.3, the Hall coefficients exhibit substantial differences in their magnitudes and temperature dependences between the amorphous and quasicrystalline phases. The alloys studied here, consisting of only simple elements, allow us to evaluate R_H on the basis of the free-electron model, using the average valence electron concentration and the measured mass density. The value of R_H for the quasicrystalline alloys with $x = 0.3$ and $Mg_{32}Al_{17}Zn_{32}$ is no longer close to the free-electron value and deviates substantially in a negative direction. Its magnitude is found to be twice as large as that for the alloys containing an amorphous phase in a matrix.

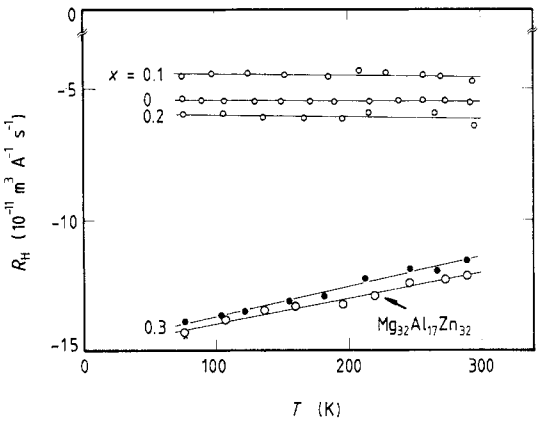

Figure 7. Temperature dependence of the Hall coefficient R_H for melt-spun $Mg_{32}Al_{17}Zn_{32}$ and $(Mg_{1-x}Al_x)_{65}Zn_{35}$ alloys.

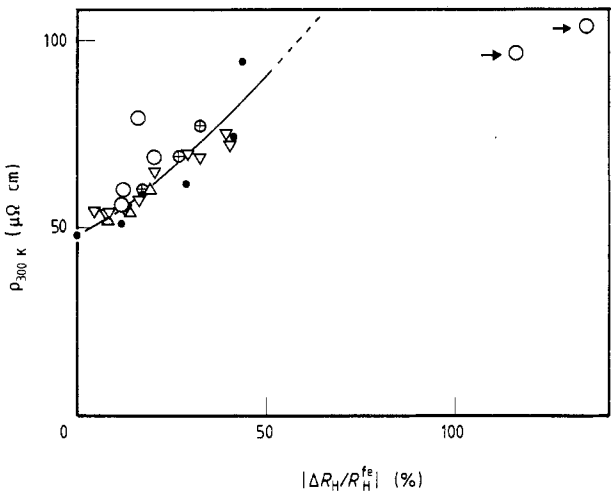

Figure 8. Resistivity against the deviation of the Hall coefficient from the free-electron value $|\Delta R_H/R_H^{fe}|$: ○, for the $Mg_{32}Al_{17}Zn_{32}$ and $(Mg_{1-x}Al_x)_{65}Zn_{35}$ alloys studied here; also using data for Mg-based amorphous alloys in the literature (after Mizutani and Matsuda 1987): ▽, Mg–Zn–Cu; ●, Mg–Zn–Ga; △, Mg–Zn–In; ⊕, Mg–Zn–Sn. The data for the quasicrystalline phase are marked by a horizontal arrow.

Mizutani and Matsuda (1987) found that the resistivity increase upon addition of a heterovalent third element to an isovalent binary amorphous alloy always accompanies the deviation of the measured Hall coefficient from the corresponding free-electron value R_H^{fe}, the parameter of which is expressed in the form of $|\Delta R_H/R_H^{fe}|$. A substantial deviation of R_H from the free-electron value is ascribed to the development of a covalent-like localised charge distribution as a result of the charge transfer between the elements having different valencies (Mizutani 1988a, b). The results are reproduced in figure 8, along with the present data including those for the quasicrystals with $x = 0.3$ and $Mg_{32}Al_{17}Zn_{32}$. It is clear that the present quasicrystals exhibit a large deviation of the Hall coefficient from the free-electron value in spite of a relatively low resistivity.

More surprisingly, the quasicrystals studied here exhibit a quite sizeable temperature dependence even at a relatively high temperature range above 77 K. The temperature coefficient of R_H (TCH), defined as $|1/R_H|(dR_H/dT)$ at 300 K, is plotted in figure 9 against the value of $|\Delta R_H/R_H^{fe}|$ for the various amorphous alloys including the present alloys. As is clear from figure 9, the temperature dependence of the Hall coefficient in

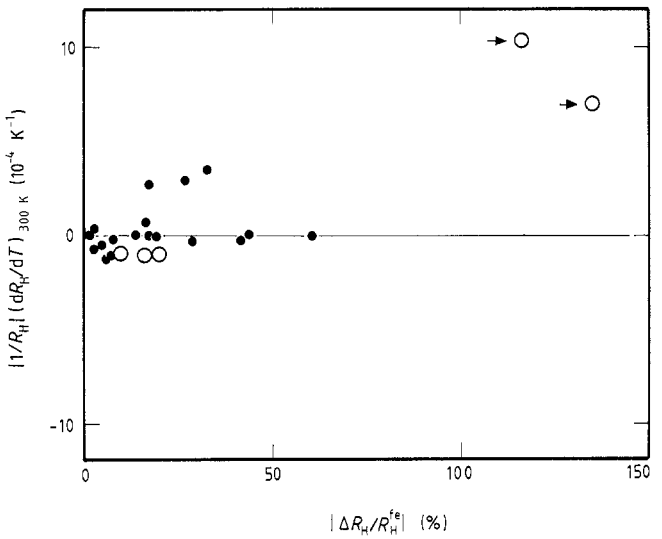

Figure 9. TCH against $|\Delta R_H/R_H^{fe}|$: ○, for the melt-spun $Mg_{32}Al_{17}Zn_{32}$ and $(Mg_{1-x}Al_x)_{65}Zn_{35}$ alloys; ●, data for Mg-based amorphous alloys in the literature (Matsuda *et al* 1984, Mizutani and Matsuda 1984). The data for the quasicrystalline phase are marked by horizontal arrows.

amorphous alloys occurs only when the value of $|\Delta R_H/R_H^{fe}|$ is increased or the resistivity is increased. The Hall coefficient in the high-resistivity disordered system is known to exhibit a square-root temperature dependence at low temperatures as a result of the enhanced electron–electron interaction (Altshuler *et al* 1980, Schulte *et al* 1984, Sakamoto *et al* 1988). As far as the non-magnetic amorphous alloys are concerned, the temperature dependence of the Hall coefficient is observed only when the resistivity reaches such a high value that the electron mean free path is limited by an average atomic distance and, hence, the ordinary Boltzmann-type transport mechanism breaks down.

Our finding on the definite temperature dependence of the Hall coefficient observed below 300 K in spite of the possession of a relatively low resistivity must be one of the most notable features characteristic of a quasicrystal. We consider that the Jones zone is well defined in the reciprocal space and that the Fermi surface interacting with the zone is no longer spherical, as opposed to that in an amorphous phase. The resemblance to the crystals in this respect would lead to a substantial deviation of the Hall coefficient from the free-electron value and its temperature dependence in spite of a relatively low resistivity. Further work should be continued along this line.

3.5. Thermo-electric power

To the best of our knowledge, the thermo-electric power of the quasicrystals has not been reported, due presumably to the difficulty in handling a sample of an extremely brittle nature. Figure 10 shows the temperature dependence of the thermo-electric power for the alloys studied here in the temperature range 77–570 K. In contrast to a small change in the resistivity as discussed in connection with figure 3 (§ 3.1), the thermo-electric power changes drastically upon crystallisation of the amorphous phase. However, it can also be seen that the transformation of the icosahedral phase into the Frank–Kasper crystal does not cause any noticeable change in the temperature dependence of the thermo-electric power (indicated by inverted triangles).

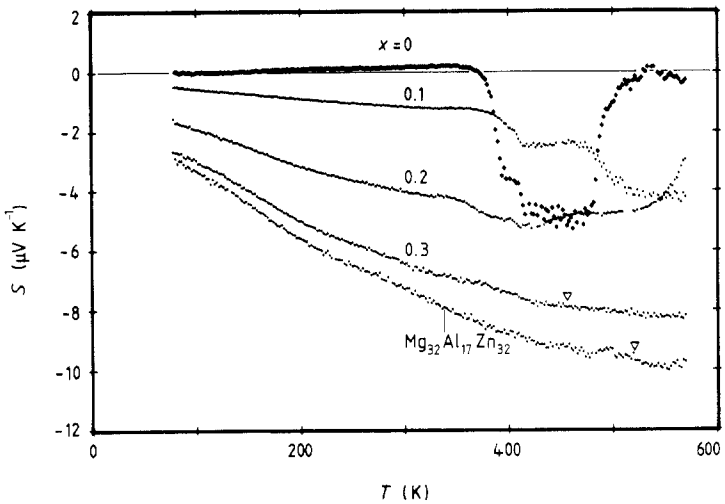

Figure 10. Temperature dependence of the thermoelectric power for melt-spun $Mg_{32}Al_{17}Zn_{32}$ and $(Mg_{1-x}Al_x)_{65}Zn_{35}$ alloys. The inverted triangles refer to the crystallisation temperature T_x.

The thermo-electric power in the quasicrystals is negative over a whole temperature range and its temperature dependence is significant. Mizutani and Matsuda (1987) have pointed out that, as far as amorphous alloys consisting of simple elements are concerned, the slope of the thermoelectric power S/T near 300 K has no relevance to the magnitude of either resistivity or $|\Delta R_H/R_H^{fe}|$. Instead, they discussed the thermo-electric parameter ξ in terms of the Faber–Ziman parameter $2k_F/K_p$, where $2k_F$ is the Fermi diameter and K_p is the wavenumber corresponding to the first peak of the structure factor. A use of the parameter $2k_F/K_p$ for the quasicrystals is, however, certainly inappropriate. Hence, it seems premature to discuss further details about the behaviour of the thermo-electric power in the quasicrystalline alloys.

Finally, it may be worthwhile mentioning that the thermo-electric power changes its slope at about 200 K with increasing Al content and its change becomes more evident when the quasicrystal single phase is formed. This might be another feature unique to the quasicrystals, since we have not observed such a change in the slope for non-magnetic amorphous alloys so far studied.

We conclude from the studies of various electron transport properties that the Hall coefficient and the thermo-electric power in the icosahedral quasicrystalline phase behave in a manner different from the amorphous phase and their temperature dependence is apparently unique to the quasicrystalline phase.

Acknowledgments

The authors are indebted to Dr K Kimura, of the Institute for Solid State Physics, University of Tokyo, and Dr Y Yamada, of the National Research Institute for Metals, for their TEM observations and for their valuable comments in the course of this project. They also thank Dr K Miura, of Aichi University of Education, for his help in the x-ray diffraction analysis associated with the crystallisation process.

References

Altshuler B L, Khmel'nitzkii D, Larkin A I and Lee P A 1980 *Phys. Rev.* B **22** 5142
Ball M D and Lloyd D J 1985 *Scr. Metall.* **19** 1065
Baxter D V, Richter R and Strom-Olsen J O 1987 *Phys. Rev.* B **35** 4819
Chen H S and Inoue A 1987 *Scr. Metall.* **21** 527
Chen H S, Phillips J C, Villars P, Kortan A R and Inoue A 1987 *Phys. Rev.* B **35** 9326
Graebner J E and Chen H S 1987 *Phys. Rev. Lett.* **58** 1945
Hafner J, Jaswal S and Tegze M 1988 *Trans. Japan Inst. Met. Suppl.* **29** 225
Inoue A, Nakano K, Bizen Y, Masumoto T and Chen H S 1988 *Japan. J. Appl. Phys.* **27** L944
Marcus M A 1986 *Phys. Rev.* B **34** 5981
Matsuda T and Mizutani U 1981 *Proc. 4th Int. Conf. Rapidly Quenched Metals* vol. 2, ed. T Masumoto and K Suzuki (Sendai: Japan Institute of Metals) pp 1315–8
—— 1982 *J. Phys. F: Met. Phys.* **12** 1877
Matsuda T, Shiotani N and Mizutani U 1984 *J. Phys. F: Met. Phys.* **14** 1193
Matsuda T, Mizutani U and Sato H 1986 *J. Phys. F: Met. Phys.* **16** 1005
Mizutani U 1988a *Mater. Sci. Eng.* **99** 165
—— 1988b *Trans. Japan Inst. Met. Suppl.* **29** 275
Mizutani U and Mizoguchi T 1981 *J. Phys. F: Met. Phys.* **11** 1385
Mizutani U and Matsuda T 1984 *J. Phys. F: Met. Phys.* **14** 2995
—— 1987 *J. Non-Cryst. Solids* **94** 345
Ramachandrarao P and Sastry G V S 1985 *Pramana* **25** L255
Sakamoto I, Yonemitsu K, Sato K and Mizutani U 1988 *J. Phys. F: Met. Phys.* **18** 2009
Sastry G V S, Rao V V, Ramachandrarao P and Anantharaman T R 1986 *Scr. Metall.* **20** 191
Shechtmann D, Blech I, Gratias D and Cahn J W 1984 *Phys. Rev. Lett.* **53** 1951
Shibuya T, Kimura K and Takeuchi S 1988 *Japan. J. Appl. Phys.* **27** 1577
Shulte A, Eckert A, Fritsch G and Luscher E 1984 *J. Phys. F: Met. Phys.* **14** 1877
Yamane H, Kimura K, Shibuya T and Takeuchi S 1987 *Mater. Sci. Forum* **22–24** 539